Electronic Supplementary Information (ESI)

Polarization-Dependent Plasmon Coupling between Au Nanorods and Au Nanospheres in Core-Satellite Nanoassemblies

Ina Jeong, Seokhyun Yun, and Sangwoon Yoon*

Department of Chemistry, Chung-Ang University

84 Heukseok-ro, Dongjak-gu, Seoul 06974, Korea

*E-mail: sangwoon@cau.ac.kr

1. Materials and Methods

1.1 Materials and Instruments

The following chemicals (without further purification) and instruments were used to synthesize AuNSs and AuNRs, and to assemble them into AuNR@AuNS nanoassemblies:

Gold(III) chloride ($HAuCl_4$, ≥99.9%, Sigma-Aldrich, U.S.A.)
Trisodium citrate (≥99.0%, Sigma-Aldrich)
Sodium borohydride ($NaBH_4$, ≥98%, Sigma-Aldrich)
Cetyltrimethylammonium bromide (CTAB, ≥99%, Sigma-Aldrich)
L-ascorbic acid (AA, 99%, Sigma-Aldrich)
Silver nitrate ($AgNO_3$, >99.9999%, Sigma-Aldrich)
(3-aminopropyl)trimethoxysilane (APTMS, 97.0%, Sigma-Aldrich)
RBS 35 solution (Sigma-Aldrich)
Sodium oleate (>97%, TCI, Japan)
Hydrochloric acid (HCl, 37%, Sigma-Aldrich)
1,8-Octanedithiol (ODT, 97%, Sigma-Aldrich)
Acetonitrile (CH_3CN, >99.5%, Daejung Chemicals, Korea)
Ethanol (≥99.9%, Duksan Chemical, Korea)
Ultrapure water (HPLC grade, J. T. Baker, U.S.A.)
Glass substrates (Marienfeld, Germany)
Rotator mixer (KRM-5, Korea Bio-Tech, Korea)
Plasma cleaner (PDC-32G-2, Harrick Plasma, U.S.A.)

To measure the properties of AuNSs, AuNRs, and AuNR@AuNS, the following instruments were used:
UV–vis spectrometer (Lambda 25, PerkinElmer, U.S.A.)
Transmission electron microscope (TEM, JEM-F200, JEOL, Japan)
Scanning electron microscope (SEM, Sigma, Carl Zeiss, Germany)
Dark-field microscope (IX-73, Olympus, Japan)
Spectrometer (Kymera 328i, Andor, U.K.)

1.2 Nanoparticle Synthesis

A. Gold Nanosphere (AuNS) Synthesis

To prepare citrate-capped AuNSs with a diameter of 37 nm, we employed the seeded growth method developed by Puntes and coworkers.[1] The amounts of reagents used in each step are summarized in **Table S1**. Stock solutions of 60 mM trisodium citrate and 25 mM $HAuCl_4$ were used in all steps. This method involves the following steps:

Step 1: Gold seeds were synthesized by boiling a mixture of trisodium citrate and water with vigorous stirring. $HAuCl_4$ was then injected into the boiling solution under stirring. The reaction proceeded for 30 min, followed by cooling the solution to 90 °C.

Step 2: $HAuCl_4$ was injected into the seed solution twice, with a 30 min interval between injections. The solution was allowed to react for 30 min.

Step 3: Trisodium citrate was added. Subsequently, $HAuCl_4$ was injected into the solution twice, with a 30 min interval between injections. The reaction was continued for 30 min. Step 3 was repeated until an extinction peak appeared at the desired wavelength.

Table S1. Sequence and amounts of added reagents for the synthesis of AuNS using the seeded growth method.

Step	Reagent	Amount (mL)
1	Water	600
	Trisodium citrate	24
	$HAuCl_4$	4
2	$HAuCl_4$	4 + 4
3	Trisodium citrate	6
	$HAuCl_4$	3 + 3
4	Trisodium citrate	5
	$HAuCl_4$	2 + 2

B. Gold Nanorod (AuNR) Synthesis

To synthesize CTAB-capped AuNRs, we modified the seeded growth method developed by Murray and coworkers.[2] For the synthesis of CTAB-capped seeds, $HAuCl_4$ (0.5 mM, 5 mL) and CTAB (0.2 M, 5 mL) were mixed in a 30 mL vial. $NaBH_4$ (6 mM, 1 mL) was added to the solution under vigorous stirring for 2 min. Subsequently, the solution was left undisturbed for 2 h in a water bath at 30 °C. To prepare the growth solution, CTAB (0.7 g) and sodium oleate (0.1234 g) were dissolved in each 12.5 mL warm water (70 °C). We mixed them and cooled them down to 30 °C slowly. We added $AgNO_3$ (4 mM, 2.4 mL) and the solution was left undisturbed for 15 min at 30 °C. Next, $HAuCl_4$ (10 mM, 2.5 mL) and water (22.5 mL) were added to the solution, which was then stirred for 90 min. The solution became colorless. HCl (37%, 0.150 mL) was added, and the mixture was stirred for 15 min. Subsequently, we added AA (64 mM, 0.125 mL) and 40 µL of the seed solution at intervals of 30 s while vigorously stirring. The solution was then left undisturbed for 12 h. For purification, the solution was centrifuged at 7000 rpm for 30 min and 5500 rpm for 20 min.

1.3 Assembly of AuNR@AuNS Core-Satellite Nanoassemblies and Preparation of Sample

We employed an assembly method developed previously by our group.[3,4] Here, we provide details of the method and the preparation of the sample for dark-field (DF) single-particle (SP) scattering spectroscopy.

***Step 1*:** The glass substrate was cut to a size of 26 × 13 mm and cleaned using RBS solutions at 90 °C for 5 min. The glass substrate was amine-coated by immersion in an ethanol solution of 1% v/v APTMS for 30 min. The mixture was transferred to ethanol and sonicated for 5 min. After rinsing with ethanol and drying with N_2 gas, the glass substrate was baked in an oven at 125 °C for 15 min to form a robust silica network of APTMS.

***Step 2*:** To adsorb core AuNRs onto the amine-coated glass substrate via electrostatic attraction, we added 0.5 mL CTAB-capped AuNRs aqueous solution to 4.5 mL acetonitrile, which converts the surface charge of AuNRs from positive to negative.[5,6] The amine-coated glass substrate was immersed in the AuNR/acetonitrile solution and shaken in a rotator mixer for 1 h. The resulting AuNR/glass substrates were washed with ethanol.

***Step 3*:** The capping ligands on the AuNRs and the amine coating on the glass substrate were removed using a plasma cleaner. The AuNRs/glass substrate was placed in the center of a plasma cleaner and operated at 18 W RF power for 20 s at 800 mTorr for air, followed by washing with water and ethanol.

***Step 4*:** To attach the dithiol linker molecules to the bare surface of the AuNRs, we immersed the glass substrate in an ethanol solution of 1 mM ODT for 1 h and then rinsed with ethanol and water.

***Step 5*:** Finally, the linker-attached AuNR/glass substrate was incubated in a citrate-capped AuNS solution for 2 h. By forming Au-S covalent bonds, the AuNSs bound to the core AuNRs.

***Step 6*:** To obtain the DF SP scattering spectra, we desorbed the AuNR@AuNS nanoassemblies from the glass substrate into 5 mL of ethanol by ultrasonication for 5 min. Subsequently, we dropcast the sample (200 μL) onto a glass slide (76 mm × 26 mm) and dried.

1.4 Characterization

We measured the properties of AuNRs, AuNSs, and AuNR@AuNS nanoassemblies using the instruments listed in **Section 1.1**. The structures of the building blocks and the final AuNR@AuNS were determined using TEM and SEM, respectively. The optical properties were measured using UV–vis spectroscopy. The extinction spectra of AuNSs in aqueous solutions were obtained. For the AuNRs and AuNR@AuNS nanoassemblies adsorbed onto the glass substrates, the substrates were immersed in a quartz cuvette, which was subsequently filled with ethanol.

1.5 Simulations

We used the finite-difference time-domain (FDTD) method to simulate the scattering spectra and charge density distributions. For the calculations, we constructed a model matching the size used in the experiments. The nanogap distance between the AuNRs and AuNSs was set to 1.3 nm, corresponding to the height of the ODT self-assembled monolayers. We employed the Norris values for the dielectric constant of gold.[7] The simulation region was enclosed by perfectly matched layer boundaries with dimensions of 1500 × 1500 × 1500 nm and a mesh size of 0.5 nm. The calculations were run with a background refractive index of 1.11 to match the experimental longitudinal plasmon mode of the AuNR at 623 nm. A simulation time was 1000 fs, and the automatic shut-off level was 10^{-8}. For the calculations of scattering cross section, a total field-scattered field source (λ = 400–1000 nm) propagated from the top of the model and excited the plasmon of the AuNR and AuNR@AuNS nanoassemblies at various polarization angles. Absorption and scattering cross section monitors were placed inside and outside the source boundaries, respectively. For the charge density distribution calculations, we used the same conditions as for the scattering spectra calculations, except for the light source. The wavelength of the incident light was fixed in longitudinal or transverse coupling mode for each nanoassembly. A charge density monitor was placed inside the source boundaries. A monitor was positioned at the horizontal cross-section of the nanoassemblies at z = 0.

2. Size Distributions of Synthesized AuNSs and AuNRs

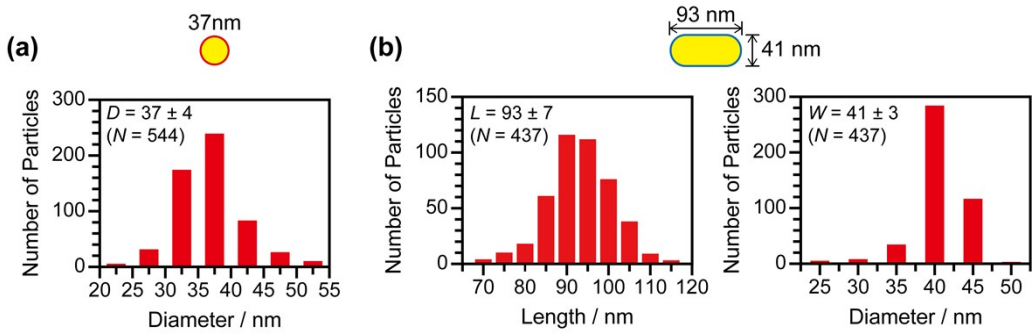

Figure S1. Size distributions of the synthesized (a) AuNSs and (b) AuNRs. The schematic dimension of each nanoparticle is provided at the top of each plot. *D*, *L*, *W* and *N* stand for diameter, length, width, and the number of particles measured for averaging, respectively.

3. Optimal Setup of a Polarizer and a Disk for Maintaining Pure Polarization

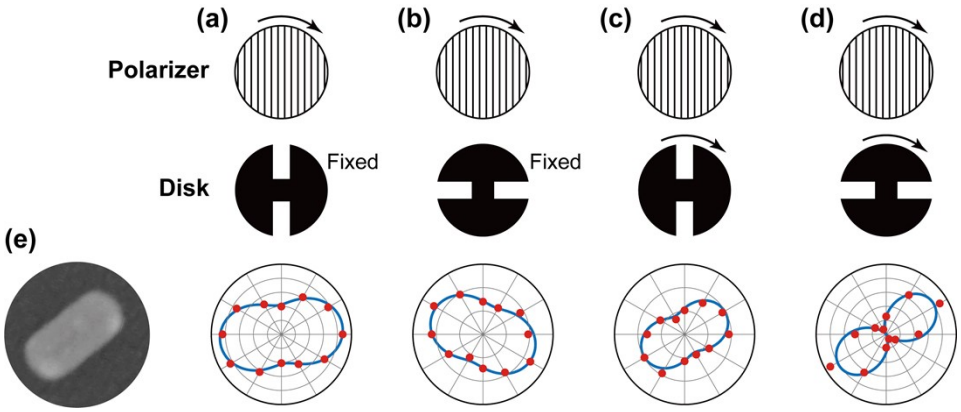

Figure S2. Search for the right combination of a linear polarizer and a cutout disk to maintain pure polarizations at the sample after a DF condenser. (a) – (d) Four different combinations of orientation and rotation were used to obtain DF SP scattering spectra for a AuNR (length = 95 nm, width = 45 nm) whose SEM image is shown in (e). Polar plots represent the scattering intensity of the longitudinal plasmon mode of the AuNR at λ = 650 nm for various polarizer angles (red circles). The polarization-dependent intensity is fitted to the $cos^2\theta$ function (blue lines). The results show that the polarization of light is mixed significantly for the setups in (a) – (c). The polarizer and disk setup in (d) prepares the most well-defined s-polarized light at the sample and accordingly excites the longitudinal mode most strongly when the polarization lines up with the long axis of the AuNR.

4. Matching the Orientation of Nanostructures with the Polarization Direction of Light

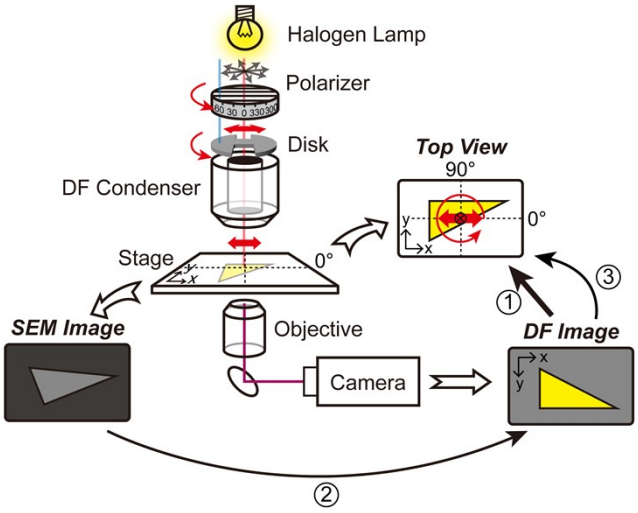

Figure S3. Experimental setup for measuring polarization-dependent single-particle scattering spectra and the procedure used to determine the orientation of a nanoparticle relative to the polarization direction of incident light.

Figure S3 illustrates our experimental setup and the procedure used to determine the orientation of the AuNR relative to the polarization direction of incident light. The key is to consider the orientation of light polarization with respect to the "top view" of the object, as this is the perspective where the light interacts with the sample. Additionally, the orientation of both the polarization and the nanoparticles must be defined within the same reference frame (e.g., lab axes).

The polarization angle is determined by marks inscribed on the rotating mount holding a linear polarizer, allowing us to know the polarization direction of the light in the lab frame as we rotate the polarizer. The orientation of the object in the same lab frame is established through a calibration process, shown as Step ① in Figure S3. In this process, we place a known object upside down on the sample stage, just as in actual DF SP scattering spectroscopy experiments using an oil immersion DF condenser. A camera mounted on the microscope captures an image of the object, which is flipped and/or rotated depending on the mirrors along the light path and the position of the camera's imaging chip. From this, we establish an operation procedure (reflection, inversion, or rotation) to recover the actual top view image from the captured image (Step ①).

During the DF SP scattering spectroscopy experiments, we record scattering spectra from single particles, whose positions are marked on the DF image. The sample is then transferred to an SEM microscope, where low-magnification SEM images are obtained. By matching the relative positions of the particles, we align the SEM image with the DF image—for example, by rotating the SEM image clockwise by 30° to align with the DF image, as shown in Figure S3. High-magnification SEM images of single particles are then processed using the same operation (Step ②).

Finally, the high-magnification SEM image of the single particle, aligned with the DF image in the previous step, is adjusted to the actual top-view orientation using the calibration procedure established in Step ① (Step ③).

5. Number of Satellite AuNSs per Core AuNR

The number of satellite AuNSs per core AuNR is determined by the relative sizes of the AuNSs (37 nm) to the AuNRs (93 nm × 41 nm) and the electrostatic repulsion between the AuNSs. Citrate-capped AuNSs adsorb onto thiol-functionalized AuNRs on glass substrates by displacing citrates with Au–S bonds. In principle, AuNSs can close-pack onto the AuNR based on their sizes. However, electrostatic repulsion between the AuNSs (due to the citrate capping on the non-adsorbed portions of the AuNSs) keeps a certain distance between them, limiting the total number of adsorbed AuNSs.

In our previous work, we demonstrated that the adsorption of citrate-capped AuNPs onto thiol-functionalized AuNPs follows Langmuir adsorption kinetics.[8] Although not perfect, we can control the number of satellites by adjusting the adsorption time and the concentration of satellite AuNPs. Under saturation conditions for both the reaction time (2 h) and the concentration (167 pM), the number of satellite AuNSs averages around 3.4, as shown in Figure S4.

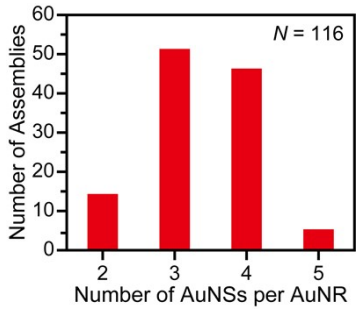

Figure S4. Distribution of the number of satellite AuNSs attached to each AuNR.

6. Further Example of Polarization-Dependent Plasmon Coupling in AuNR@AuNS

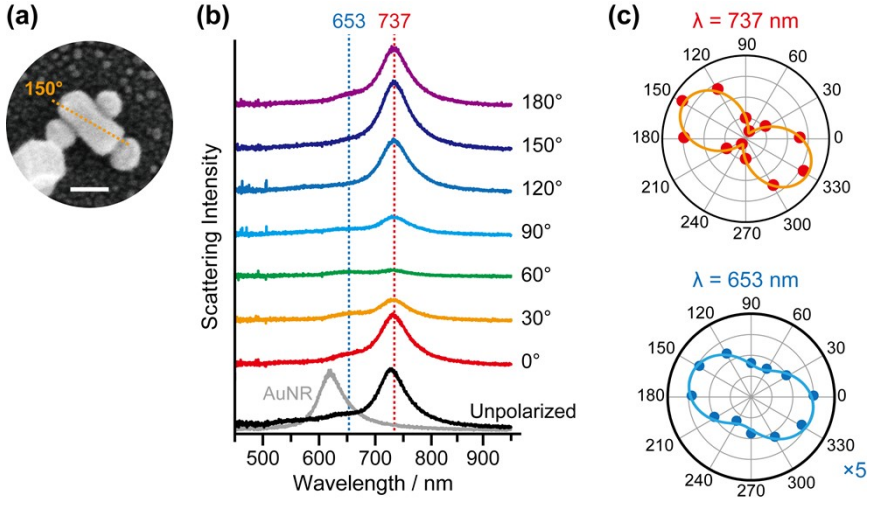

Figure S5. Polarization-dependent DF SP scattering spectra of the AuNR@AuNS nanoassembly. (a) SEM image of the AuNR@AuNS nanoassembly used in the experiment. The orange dotted lines represent the polarization angles of the incident light that yield the largest intensities of the longitudinal plasmon coupling mode peak at λ = 737 nm. The scale bar represents 50 nm. (b) DF SP scattering spectra as the polarization of the incident light changes. The peaks at 737 and 653 nm are attributed to the longitudinal and transverse plasmon coupling modes,

respectively. For comparison, the DF SP scattering spectrum of AuNR@AuNS using unpolarized light (black line) and that of the AuNR monomer (grey line) are included. (c) Polar plots showing the scattering intensities at 737 nm (red circles) and 653 nm (blue circles) plotted against the polarization angle and fitted to the $cos^2\theta$ function (solid lines). The fitting indicates the largest scattering intensity of the longitudinal plasmon coupling mode at a polarization angle of 150° (orange line). The transverse plasmon coupling is not as directional as the longitudinal plasmon coupling, as indicated by the thick waist of the $cos^2\theta$ function (cyan line). Note that the square pillar structure in the lower-left corner of the SEM image in (a) is a contaminant (a piece of broken glass) that was accidently introduced during the SEM sampling process. Consequently, it does not affect the DF SP scattering spectra. Additionally, the small particles in the SEM image are Pt grains from the Pt coating used for SEM measurements.

References

(1) Bastús, N. G.; Comenge, J.; Puntes, V. Kinetically Controlled Seeded Growth Synthesis of Citrate-Stabilized Gold Nanoparticles of up to 200 nm: Size Focusing Versus Ostwald Ripening. *Langmuir* **2011**, *27*, 11098-11105.

(2) Ye, X. C.; Zheng, C.; Chen, J.; Gao, Y. Z.; Murray, C. B. Using Binary Surfactant Mixtures to Simultaneously Improve the Dimensional Tunability and Monodispersity in the Seeded Growth of Gold Nanorods. *Nano Lett.* **2013**, *13*, 765.

(3) Trinh, H. D.; Kim, S.; Yun, S.; Huynh, L. T. M.; Yoon, S. Combinatorial Approach to Find Nanoparticle Assemblies with Maximum Surface-Enhanced Raman Scattering. *ACS Appl. Mater. Interfaces* **2024**, *16*, 1805-1814.

(4) Yun, S.; Yoon, S. Mode-Selective Plasmon Coupling between Au Nanorods and Au Nanospheres. *J. Phys. Chem. Lett.* **2023**, *14*, 10225-10232.

(5) Pramod, P.; Thomas, K. G. Plasmon Coupling in Dimers of Au Nanorods. *Adv. Mater.* **2008**, *20*, 4300-4305.

(6) Pramod, P.; Joseph, S. T. S.; Thomas, K. G. Preferential End Functionalization of Au Nanorods through Electrostatic Interactions. *J. Am. Chem. Soc.* **2007**, *129*, 6712-6713.

(7) McPeak, K. M.; Jayanti, S. V.; Kress, S. J. P.; Meyer, S.; Lotti, S.; Rossinelli, A.; Norris, D. J. Plasmonic Films Can Easily Be Better: Rules and Recipes. *ACS Photonics* **2015**, *2*, 326-333.

(8) Yoon, J. H.; Yoon, S. Effects of the Number of Satellites on Surface Plasmon Coupling of Core-Satellite Nanoassemblies. *Bull. Korean Chem. Soc.* **2013**, *34*, 33-34.